ARTICLES

Comments on the ^{27}Al NMR Visibility of Aluminas

H. Kraus, M. Müller, and R. Prins*

Laboratory for Technical Chemistry, Swiss Federal Institute of Technology, 8092 Zürich, Switzerland

A. P. M. Kentgens

N.S.R. Institute for Molecular Structure, Design and Synthesis, National HF-NMR Facility, University of Nijmegen, Toernooiveld 1, 6525 ED Nijmegen, The Netherlands

Received: September 5, 1997; In Final Form: December 10, 1997

The influence of surface area, paramagnetic impurities, and spinning speed on the ^{27}Al MAS NMR visibility in a number of γ- and η-Al_2O_3 samples was investigated. It is shown that magic angle spinning (MAS) under typical conditions (~10 kHz spinning speed at a 9.4 T field) is insufficient to resolve all aluminium sites in the samples. Since, in general, the number of strongly distorted sites in aluminas increases with the surface area, the ^{27}Al MAS NMR signal intensities at 10−15 kHz spinning decrease. Differences between γ- and η-Al_2O_3 intensities are explained by their structural differences, causing weaker distortions in η- than in γ-Al_2O_3. At spinning speeds up to 29 kHz all aluminium is accounted for in the MAS spectra. Paramagnetic iron impurities up to 1440 ppm do not have a significant influence on the ^{27}Al MAS NMR visibility of the investigated samples.

Introduction

Aluminas, especially γ-Al_2O_3, are widely used as catalysts and catalyst supports. A technique that recently gained increasing popularity for characterization of γ-Al_2O_3 is solid-state ^{27}Al NMR spectroscopy. Unfortunately, it was observed that a significant fraction of the aluminum atoms in γ-Al_2O_3 escapes detection by NMR. Already in 1960 O'Reilly measured γ-Al_2O_3 samples on a 28 MHz cw-spectrometer.[1] He found a correlation between aluminum visibility and surface area of the materials. According to his study, assuming that the quadrupole interaction of Al in the first two layers is too large to be observed, a sample with a surface area of 230 m^2/g should have an aluminum visibility of 70% for the center $^1/_2 \leftrightarrow -^1/_2$ transition. More recently, Huggins and Ellis[2] observed 55% of the Al atoms for a material with a surface of 220 m^2/g. They hold dynamic processes at the surface, inducing a very efficient quadrupolar relaxation path, responsible for the signal loss. Their spectra were recorded on a 400-MHz spectrometer under static conditions. Our own recent ^{27}Al MAS NMR measurements on a 500-MHz spectrometer with a spinning frequency of about 13 kHz showed that approximately 90% of the Al atoms in a γ-Al_2O_3 with a surface area of 230 m^2/g can be detected.[3] In addition, upon impregnation of γ-Al_2O_3 with phosphate or molybdate, the formation of new surface compounds was observed, which had an influence on the Al visibility as well.[3] In order to elucidate the effects causing the signal losses, a series of γ-Al_2O_3 samples was studied, concentrating on surface variations, the effect of paramagnetic impurities, and experimental conditions.

Experimental Section

Samples. The following samples were commercially obtained: Condea (Tonerde Granulate from Condea Chemie GmbH), JM (γ-Al_2O_3 99.99% from Johnson Matthey), and AC (alumina blanks from American Cyanamid). Some samples were provided by commercial suppliers: Ketjen (Ketjen CK300) and Puralox (from Condea Chemie GmbH). Two samples were prepared from gelatinous boehmite, provided by Shell. Direct calcination of this gelatinous boehmite at 450 °C for about 20 h resulted in the sample called Boe-C. A highly crystalline boehmite was obtained by hydrothermal treatment of the gelatinous boehmite at 220 °C for 24 h in an autoclave. Calcination of the crystalline boehmite at 550 °C for 20 h gave sample CrBoe-C. Three samples were prepared by hydrolyzing 2.5 g of $Al(C_3H_7O)_3$ in 50 mL of water by stirring the solution for 8 h at 80 °C. The resulting suspension was cooled and filtered, and the filtrate was washed several times with water. The filter cake was dried at 120 °C for 6 h to give gelatinous boehmite. γ-Al_2O_3 samples Syn and Syn-Fe were then obtained by calcination of the different boehmite samples for 20 h at 450 °C. For preparation of the Syn-Fe sample, the water used for hydrolysis contained 4.6 mg of $Fe(NO_3)_3 \cdot 9H_2O$. Two samples of α-Al_2O_3 were used as an intensity reference. The first (Alpha-1) was obtained from R & L Slaughter ("Calcinet"), the second (Alpha-2) was prepared by calcination of the Condea γ-Al_2O_3 at 1300 °C for 12 h. Finally, two η-Al_2O_3 were included in the study. A sample called Eta-1 was purchased from Condea Chemie GmbH, whereas sample Eta-2 was obtained by calcination of a bayerite (Condea Chemie GmbH) at 450 °C for 20 h. BET surface areas, pore volumes, iron content, and Al_2O_3 content for each sample are given in Table

S1089-5647(97)02909-X CCC: $15.00
Published on Web 04/23/1998

TABLE 1

sample	BET surface area (m^2/g)	pore volume (cm^3/g)	Al_2O_3 content (%)	Fe content (ppm)	^{27}Al MAS NMR visibility[a] (%)	static ^{27}Al NMR visibility (%)
Cr-Boe-C	57	0.30	98.6	118	85	109
JM	113	0.50	89.2	6	94	111
AC	201	0.50	92.1	70	82	97
Puralox	214	0.54	95.1	80	78	98
Condea	230	0.53	88.9	110	78	107
Ketjen	263	0.65	94.0	179	73	95
Syn	289	0.45	96.3	24	73	93
Boe-C	311	0.42	99.3	126	82	95
Syn-Fe	321	0.47	91.4	1440	70	102
Eta-1	298	0.36	92.9	82	88	90
Eta-2	432	0.35	87.1	70	81	97
Alpha-1	<10		100		97	100[b]
Alpha-2	<10		100		103	100

[a] Measured at 9.4 T using a 12.5-kHz spinning speed. [b] The average intensity of the two α-Al_2O_3 samples was set at 100 for the static measurements.

1. The Al_2O_3 content can be calculated via the Al content as measured by atomic absorption spectroscopy. The missing weight percent are mainly due to water as checked with thermogravimetric analysis. Each sample was controlled by X-ray diffraction (Siemens D5000) for the correct alumina phase (α, γ, or η).

NMR Measurements. ^{27}Al MAS and static single-pulse NMR spectra were obtained on a Bruker AMX400 spectrometer equipped with a 4-mm Bruker MAS probehead. The rf-field strength was 50 kHz using 0.5-μs excitation pulses ensuring quantifiability of the spectra. Each sample was measured statically and with spinning frequencies of 10 and 12.5 kHz. Recycle times were set long enough to obtain fully relaxed spectra (≥1 s for γ-Al_2O_3 and ≥10 s for α-Al_2O_3). Chemical shifts are referenced with respect to 0.1 M $Al(NO_3)_3$. For a quantitative comparison, the intensity of the center bands was integrated. In order to correct for the satellite transition contribution to the center band in MAS spectra, the average intensity of the first spinning sideband on each side of the center band was subtracted from the center band intensity. Furthermore, the intensity was corrected for dead time effects. In static spectra baseline rolling was observed. Therefore the static spectra were left shifted and corrected by linear back-projection to overcome the overall dead time. No special sample pretreatment or sealing procedure was used for the NMR experiments.

^{27}Al NMR spectra of the samples Cr-Boe-C, JM, Condea, Syn-Fe, and Eta-1 were run independently on a Chemagnetics CMX Infinity 400-MHz spectrometer. Spectra were obtained in a Chemagnetics 2.5-mm MAS probehead with an rf-field strength of 80 kHz and an excitation pulse length of 0.3 μs. The spectra were run statically and at spinning speeds of 10, 20, and 29 kHz. Back-projection was used to overcome dead time effects.

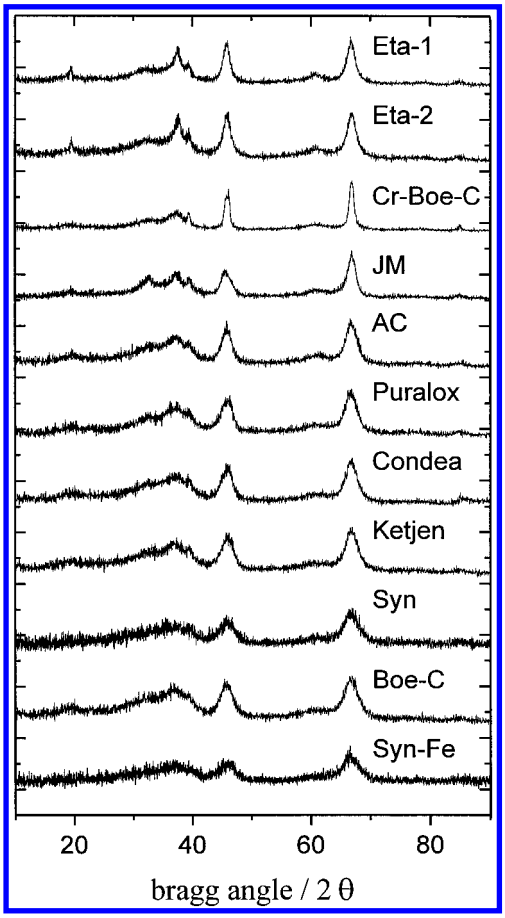

Figure 1. X-ray powder diffractograms of γ- and η-aluminas ordered, from top to bottom, according to increasing surface area of the samples.

Results and Discussion

γ- and η-aluminas are so-called transition aluminas, which are mostly obtained by (partial) dehydroxylation of boehmite (γ-AlOOH) and bayerite (α-$Al(OH)_3$), respectively. The crystal lattices of both aluminas are described as being of the spinel type, consisting of cubic close-packed layers of oxygen ions with the cations distributed over the tetrahedral and octahedral interstices.[4] In the normal $M^{3+}M^{2+}$ (AB_2O_4) spinel, 32 oxygen anions and 24 cations make up the unit cell. However, only $21^1/_3$ Al^{3+} ions are available for the cation positions in γ- and η-alumina. Thus, their spinel-type lattices contain cation vacancies. This may be one of the reasons for the distortions of the spinel structure observed for the two types of alumina. γ-Al_2O_3 has a fairly well-ordered oxygen sublattice and strongly tetragonally deformed aluminum sublattices. In contrast, the structure of η-Al_2O_3 is only somewhat tetragonally deformed, but with a less well-ordered oxygen sublattice.[4,5] The structural disorder is reflected in a diffuse XRD powder pattern, exhibiting small differences for the two types of alumina.[5,6] X-ray powder diffractograms of the γ- and η-aluminas used in this study are displayed in Figure 1. The diffractograms are ordered according to the surface area of the samples, separately for γ-Al_2O_3 and η-Al_2O_3. Samples with the highest surface area are displayed at the bottom of each series. As expected, γ- and η-aluminas are clearly distinguishable from their X-ray diffractograms. Especially, the signals at about $2\theta = 19°$ and $2\theta = 37°$ in

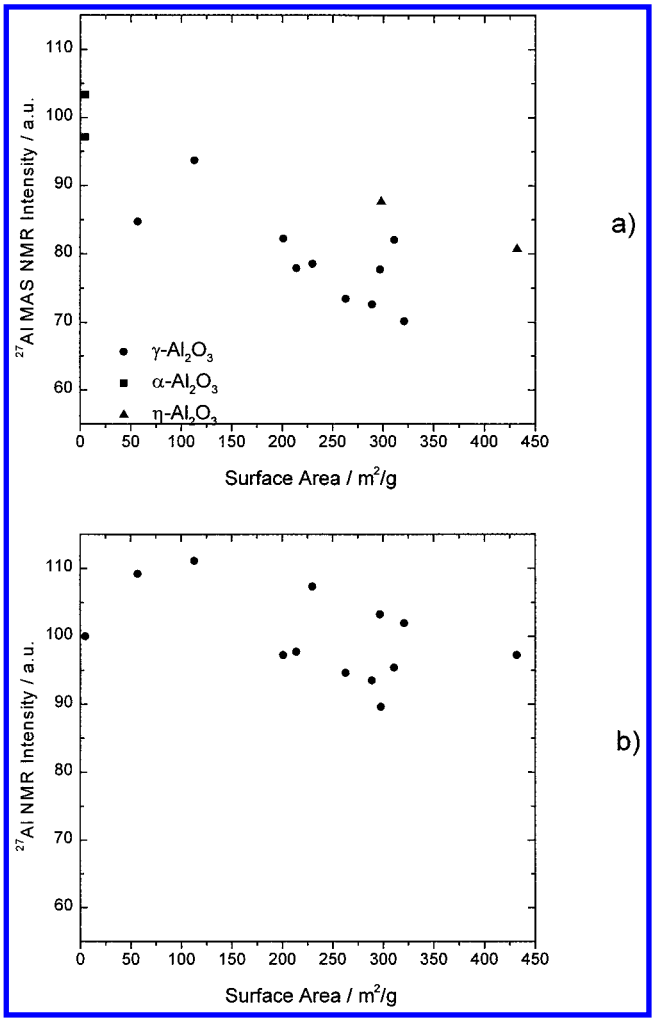

Figure 2. Center band intensity of ^{27}Al MAS NMR spectra of γ- and η-Al_2O_3 samples plotted against surface area: (a) MAS spectra at 12.5 kHz spinning speed, (b) static spectra.

η-Al_2O_3 are much sharper and more pronounced than in γ-Al_2O_3. Another observation is that the degree of ordering increases with decreasing surface area. The X-ray diffractograms of the two α-Al_2O_3 samples also compared well with the published data.

Having thus established that all samples are of the right phase, they were used for the NMR experiments. The quantitative analyses of the static and 12.5-kHz MAS spectra are summarized in Table 1 and Figure 2. As can be seen, the aluminium is accounted for in the static spectra, taking the accuracy (±6%) of the integration into account. One might argue that there is a small trend to lower intensities with increasing surface areas. This effect is small, however. We certainly do not see the strong decrease in signal intensity reported by O'Reilly[1] and Huggins and Ellis.[2] Furthermore, we could not reproduce the observation of Huggins and Ellis that any lost intensity, which they claimed to be due to proton dynamics, can be regained by lowering the temperature. MAS experiments at temperatures down to −100 °C give no other signal gain than that expected on the basis of the Boltzmann factor. Moreover, no change in line shape was observed.

Addition of paramagnetic iron impurities up to 1440 ppm has no effect on the detectability of aluminium. In a previous study of a series of α-Al_2O_3 samples, we found that small Fe impurities in commercial samples reduce the effective relaxation delay but not the "visibility" of aluminium. Only high (up to 0.5 wt %) concentrations of Fe_2O_3 and Cr_2O_3 in natural samples led to a significant signal loss.[7]

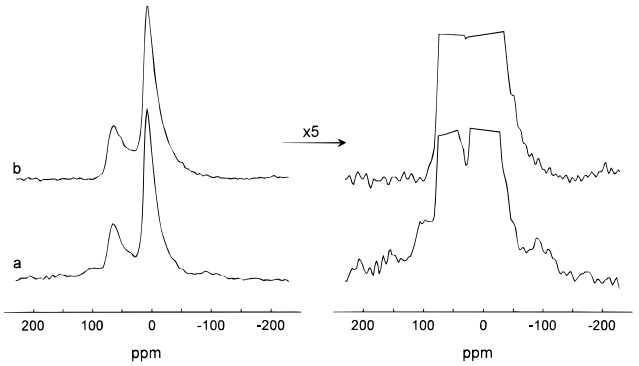

Figure 3. ^{27}Al MAS NMR spectra of Syn-Fe obtained at a spinning speed of (a) 10 kHz and (b) 29 kHz. The lines seem narrower in the 10-kHz spectrum, but there is an unresolved hump underneath the resonances. The lines in the 29-kHz spectrum are broader, but the baseline is perfectly flat. In this spectrum the rotation frequency exceeds the second-order quadrupolar broadening of all sites in the sample.

The question that remains to be answered is why the amount of observed aluminium is significantly lower in the MAS spectra as compared to the static data. Moreover, in a previous study we observed approximately 90% of the aluminum atoms of the Condea sample (230 m^2/g) in a MAS measurement at 11.7 T using a spinning speed of 12.5 kHz,[3] whereas in the present study (9.4 T, 12.5 kHz) only 78% is detected. A possible reason might be an insufficient averaging of the second-order quadrupolar couplings by magic angle spinning, for some of the sites in the samples, under the conditions used. These sites with large quadrupole coupling only contribute weakly to the center line as their MAS center band and spinning sidebands are not well-separated. Thus their intensity is smeared out substantially. With increasing spinning speed more and more of these sites are narrowed to their residual MAS line width, thus contributing to the observed center band making it effectively broader. Such effects have been reported by Sato et al.[8] This process continues up to the point were the MAS frequency exceeds the line width of the site with the largest QCC in the distribution. To investigate this effect, we decided to monitor the line width and Al visibility as a function of spinning speed in a 2.5-mm fast MAS probehead that has recently become available. Spectra were taken statically and at spinning speeds of 10, 20, and 29 kHz. Figure 3 shows the spectrum of Syn-Fe at 10 and 29 kHz. The line width is clearly narrower in the spectrum taken at 10 kHz; a broad unresolved hump and overlap of spinning sidebands with the center band is visible, however, in the inlayed spectrum. The baseline is perfectly flat in the spectrum taken at 29 kHz. For all investigated samples, it appeared that aluminium is visible in the spectra taken with a spinning exceeding 20 kHz. These observations prove that distributions in quadrupole coupling constant in the alumina samples are very large, and high spinning speeds (>20 kHz at 9.4 T) are essential for an accurate analysis of the spectra. Indeed, our previous MQMAS experiments[3] showed that there is a large distribution in both isotropic chemical shift and quadrupole parameters of aluminium atoms in γ-Al_2O_3. This large distribution gives rise to the low-frequency tails of the resonance. Inspection of the 29-kHz spectra shows that the line widths are different for all samples, reflecting subtle differences in the Al ordering in the various aluminas. For the octahedrally coordinated aluminium (Al(VI)), we observed the following increase in line width: Eta-1 ∼ Condea < JM ∼ Cr-Boe-C < Syn-Fe. For the linewidth of the tetrahedrally coordinated Al, we found Eta-1

< Condea ∼ JM < Cr-Boe-C ∼ Syn-Fe. It can be concluded that the distribution in chemical shift and quadrupole coupling constant in η-Al_2O_3 is smaller than in γ-Al_2O_3. This suggests a higher degree of order in the alumina sublattice for η-Al_2O_3. This corresponds well with findings from XRD and neutron diffraction by Zhou and Snyder.[5] They found 13% of the aluminium atoms in an η-Al_2O_3 of about 300 m^2/g and 25% of the aluminum atoms in a γ-Al_2O_3 of about 200 m^2/g in a very distorted surrounding and proposed that these Al atoms in distorted surroundings are located in the surface layer. Thus their number is increasing with surface area for both types of aluminas. These results give credit to the proposal of O'Reilly[1] that part of the aluminium atoms are experiencing large quadrupole couplings owing to distortions in the alumina surface layer. We find, however, that all these sites are observable under the appropriate experimental conditions. It should be noted that a very recent study by Maciel and co-workers[9] of pseudo Boehmite samples also showed that all aluminium is visible in MAS spectra obtained at high field (14.1 T) and fast MAS speed (16−17 kHz). They also attribute the lack of Al visibility in earlier studies to the limited technical conditions in earlier work.

Taking these considerations into account, we expect the line width of the γ-Al_2O_3 samples to increase with increasing surface area, which is indeed generally observed. The Cr-Boe-C sample forms a marked exception, however, because it has the lowest surface area of all samples in this study, but displays among the largest line widths and a rather low visibility at 10-kHz spinning speed. Its aluminium sublattice seems to be more disordered as compared to other samples with low surface area. Thus surface area as measured by BET is not the only parameter important for the Al ordering. On the other hand, the X-ray diffractogram of the sample (Figure 1) confirms the rather good ordering of the oxygen sublattice, well-correlated to the low surface area.

In order to gain more insight in the alumina structure, it is of further interest to determine the ratio of aluminium in a tetrahedral and an octahedral coordination.[10−12] The MAS spectra taken at 29 kHz show, however, that the two resonances are not yet completely resolved. Indeed, MQMAS experiments on some of the samples show that the tail of the Al(IV) resonance runs down to ∼0 ppm and thus significantly overlaps with the Al(VI) resonance. The determination of the Al(IV)/Al(VI) ratio and the amount of disorder experienced by both sites can only be obtained by a detailed simulation of both MAS and MQMAS spectra taking the distribution in chemical shifts and quadrupole parameters into account. Line shape analysis such as presented by Meinhold et al.[13] and Jaeger et al.[14] should give more insight into the nature of the distributions of the quadrupole parameters. Obviously these spectra have to be taken at appropriately high spinning speeds. Such investigations are in progress.

References and Notes

(1) O'Reilly, D. E. *Adv. Catal.* **1960**, *12*, 31.
(2) Huggins, B. A.; Ellis, P. D. *J. Am. Chem. Soc.* **1992**, *114*, 2098.
(3) Kraus, H.; Prins, R.; Kentgens, A. P. M. *J. Phys. Chem.* **1996**, *100*, 16337.
(4) Lippens, B. C. Thesis, Technical University of Delft, The Netherlands, 1961.
(5) Zhou, R-S.; Snyder, R. L. *Acta Crystallogr. B* **1991**, *47*, 617.
(6) Wefers, K.; Misra, C. *Alcoa Technical Paper*; Alcoa Laboratories: Pittsburg, PA, 1987; No. 19 revised.
(7) Kentgens, A. P. M.; Bos, A.; Dirken, P. J. *Solid State Nucl. Magn. Reson.* **1994**, *3*, 315.
(8) Sato, R. K.; McMillan, P. F.; Dennison, P.; Dupree, R. *J. Phys. Chem.* **1991**, *95*, 4483.
(9) Fitzgerald, J. J.; Piedra, G.; Dec, S. F.; Seger, M.; Maciel, G. E. *J. Am. Chem. Soc.* **1997**, *119*, 7832.
(10) Dupree, R.; Farnan, I.; Forty, A. J.; El-Mashri, S; Bottyan, L. *J. Phys.* **1985**, *46* (C-8), 113.
(11) John, C. S.; Alma, N. C. M.; Hays, G. R. *Appl. Catal.* **1983**, *6*, 341.
(12) Lee, M.-H.; Cheng, C.-F.; Heine, V.; Klinowski, J. *Chem. Phys. Lett.* **1997**, 265, 673.
(13) Meinhold, R. H.; Slade, R. C. T.; Newman, R. H. *Appl. Magn. Reson.* **1993**, *4*, 121.
(14) Jaeger, C.; Kunath, G; Losso, P; Scheler, G. *Solid State Nucl. Magn. Reson.* **1993**, 2, 73.